Ultrahigh-temperature microwave annealing of Al^+- and P^+-implanted 4*H*-SiC

Siddarth G. Sundaresan and Mulpuri V. Rao[a)]
Department of Electrical and Computer Engineering, George Mason University, Fairfax, Virginia 22030

Yong-lai Tian
LT Technologies, Fairfax, Virginia 22033

Mark C. Ridgway
Department of Electronic Materials Engineering, Australian National University, Canberra ACT 0200, Australia

John A. Schreifels
Department of Chemistry and Biochemistry, George Mason University, Fairfax, Virginia 22030

Joseph J. Kopanski
Semiconductor Electronics Division, National Institute of Standards and Technology, Gaithersburg, Maryland 20899

(Received 20 August 2006; accepted 6 February 2007; published online 12 April 2007)

In this work, an ultrafast solid-state microwave annealing has been performed, in the temperature range of 1700–2120 °C on Al^+- and P^+-implanted 4*H*-SiC. The solid-state microwave system used in this study is capable of raising the SiC sample temperatures to extremely high values, at heating rates of ~600 °C/s. The samples were annealed for 5–60 s in a pure nitrogen ambient. Atomic force microscopy performed on the annealed samples indicated a smooth surface with a rms roughness of 1.4 nm for 5×5 μm^2 scans even for microwave annealing at 2050 °C for 30 s. Auger sputter profiling revealed a <7 nm thick surface layer composed primarily of silicon, oxygen, and nitrogen for the samples annealed in N_2, at annealing temperatures up to 2100 °C. X-ray photoelectron spectroscopy revealed that this surface layer is mainly composed of silicon oxide and silicon nitride. Secondary ion mass spectrometry depth profiling confirmed almost no dopant in diffusion after microwave annealing at 2100 °C for 15 s. However, a sublimation of ~100 nm of the surface SiC layer was observed for 15 s annealing at 2100 °C. Rutherford backscattering spectra revealed a lattice damage-free SiC material after microwave annealing at 2050 °C for 15 s, with scattering yields near the virgin SiC material. Van der Pauw–Hall measurements have revealed sheet resistance values as low as 2.4 kΩ/□ for Al^+-implanted material annealed at 2100 °C for 15 s and 14 Ω/□ for the P^+-implanted material annealed at 1950 °C for 30 s. The highest electron and hole mobilities measured in this work were 100 and 6.8 cm^2/V s, respectively, for the P^+- and Al^+-implanted materials. © *2007 American Institute of Physics*. [DOI: 10.1063/1.2717016]

I. INTRODUCTION

The 4*H* polytype of silicon carbide (SiC) has received immense interest over the past decade for making high-power electronic devices with a wide range of breakdown voltages (600 V–20 kV), as well as for making high frequency metal-semiconductor field-effect transistors (MESFETs).[1,2] This is due to the fact that the 4*H*-SiC has the largest band gap (3.2 eV) and highest electron mobility of all SiC polytypes.[3,4] Ion implantation remains the only planar, selective area doping technology available for SiC, which always needs to be followed by high-temperature annealing (>1500 °C).[5–7] Postimplant annealing activates the implanted dopants and heals the implant-generated lattice damage. The optimization of the postimplant annealing process (especially for acceptor dopants) needs further development. Ideally, what one expects from postimplant annealing is a low sheet resistance, which results from a combination of low lattice damage (high carrier mobility) and high carrier concentration. A low implant layer sheet resistance leads to low contact and channel region resistances, consequently decreasing the power consumption in high-power devices.

The SiC sublimation limits the maximum annealing temperature and consequently the lowest possible sheet resistance obtainable for conventional annealing. A solid-state microwave rapid thermal annealing (RTA) system developed by LT Technologies is attractive for postimplant annealing of SiC.[8] This microwave RTA system is capable of providing a temperature rise rate of >600 °C/s and a fall rate of 400 °C/s, enabling a short duration high-temperature (>1800 °C) annealing of SiC. Using this microwave RTA system, promising lattice quality and electrical activation results were obtained in our earlier work;[8] however, microwave anneals were performed in air in that work, limiting the maximum annealing temperature and the anneal time due to

[a)]Author to whom correspondence should be addressed; present address: 4400 University Dr, ST-II, No. 217, Fairfax, VA 22030; electronic mail: rmulpuri@gmu.edu

Report Documentation Page

Form Approved
OMB No. 0704-0188

1. REPORT DATE	2. REPORT TYPE	3. DATES COVERED
02 SEP 2007		**01-08-2006 to 31-07-2007**

4. TITLE AND SUBTITLE	5a. CONTRACT NUMBER
Ultrahigh-Temperature Microwave Annealing of A1+- and P+-Implanted 4H-SiC	5b. GRANT NUMBER
	5c. PROGRAM ELEMENT NUMBER
6. AUTHOR(S)	5d. PROJECT NUMBER
	5e. TASK NUMBER
	5f. WORK UNIT NUMBER
7. PERFORMING ORGANIZATION NAME(S) AND ADDRESS(ES) **George Mason University,Office of Sponsored Programs,4400 University Dr., MSN 4C6,Fairfax,VA,27709-2211**	8. PERFORMING ORGANIZATION REPORT NUMBER **; 46232-MS-2**
9. SPONSORING/MONITORING AGENCY NAME(S) AND ADDRESS(ES) **US Army Research Office, P.O. Box 2211, Research Triangle Park, NC, 27709-2211**	10. SPONSOR/MONITOR'S ACRONYM(S)
	11. SPONSOR/MONITOR'S REPORT NUMBER(S) **46232-MS-2**

12. DISTRIBUTION/AVAILABILITY STATEMENT
Approved for public release; distribution unlimited

13. SUPPLEMENTARY NOTES
Federal Purpose Rights

14. ABSTRACT

15. SUBJECT TERMS

16. SECURITY CLASSIFICATION OF:			17. LIMITATION OF ABSTRACT	18. NUMBER OF PAGES	19a. NAME OF RESPONSIBLE PERSON
a. REPORT	b. ABSTRACT	c. THIS PAGE			
unclassified	**unclassified**	**unclassified**	**Same as Report (SAR)**	**7**	

TABLE I. Implant schedules used in this study.

Species	Implant energy (keV)	Implant dose (cm^{-2})
Aluminum	10	4.5×10^{15}
	25	7×10^{14}
	40	6.7×10^{14}
	100	1.6×10^{15}
	200	2×10^{15}
	325	1.8×10^{15}
	400	2.2×10^{15}
Phosphorus	10	5×10^{14}
	20	5×10^{15}
	60	9×10^{14}
	100	2.2×10^{15}
	200	4.5×10^{15}

the growth of a thick (>100 nm) oxide layer during high-temperature (>1850 °C) annealing. The limitations in the annealing temperature and time compromised the optimum electrical properties possible by the solid-state microwave annealing. In this work, we have performed solid-state microwave annealing on phosphorus and aluminum ion-implanted 4*H*-SiC in controlled inert atmospheres of N_2, Ar, or Xe, to prevent surface oxidation of SiC. Phosphorus is the preferred *n*-type dopant in SiC because of its higher solubility limit in SiC than that of nitrogen, which cannot be incorporated in excess of 3×10^{19} cm^{-3} due to precipitation during postimplantation annealing.[9,10] Aluminum is a popular acceptor in SiC due to its lower ionization energy compared to other acceptors such as B and Ga.[11] In this work, annealing in an inert ambient solved the oxidation problem, allowing for high-temperature (~2100 °C) annealing and yielding very low sheet resistances and very high carrier mobilities in implanted 4*H*-SiC. The principal aim of this work is obtaining near virgin lattice quality and high sheet carrier concentration in implanted 4*H*-SiC using high annealing temperatures for 5–60 s.

In this paper, we report on the surface morphology, surface composition and stoichiometry, implant depth profile, and electrical and lattice quality properties of Al^+ and P^+ ion-implanted 4*H*-SiC annealed by a solid-state microwave technique in an inert ambient for 5–60 s at temperatures as high as 2120 °C.

II. EXPERIMENT

Multiple-energy Al^+ and P^+ implant schedules performed into semi-insulating (SI) 4*H*-SiC are given in Table I. The Al^+ implant was performed into an on-axis wafer with a 7° tilt and the P^+ implant was performed into an 8° off-axis (toward [11-20]) wafer. Both the Al^+ and P^+ implants were performed at 500 °C. The P^+ and Al^+ implants were designed to obtain a uniform implant concentration of 2×10^{20} cm^{-3} to a depth of ~0.3 and 0.5 μm, respectively, except at the surface. The lowest energy implant was designed to obtain a decade higher surface doping concentration than the rest of the depth to obtain a very low Ohmic contact resistance.

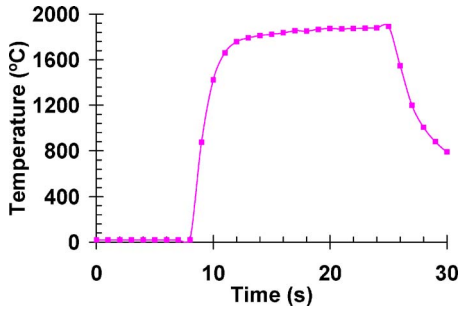

FIG. 1. (Color online) A typical temperature-time cycle depicting the ultrafast heating and cooling rates of the solid-state microwave annealing system.

A detailed description of the solid-state microwave annealing system used in this work is provided elsewhere.[8] Since SI SiC samples were used in this study, during microwave annealing, an *in-situ* doped conductive 4*H*-SiC sample was placed beneath the implanted SI sample. The conductive sample served as the susceptor for efficiently heating the SI sample of interest. In this work, microwave annealing was mainly performed in a controlled atmosphere of 100% nitrogen. In addition to nitrogen, microwave annealing was attempted in atmospheres of other inert gases such as helium, argon, and xenon. However, these latter gases were found to ionize (generating arcing) due to the intense microwave field in the vicinity of the SiC sample. The annealing temperatures used in this work ranged from 1800–2120 °C for the aluminum-implanted samples and 1700–1950 °C for the phosphorus-implanted samples. The annealing durations for both aluminum and phosphorus implants varied from 5 to 60 s. A typical temperature-time cycle for 1900 °C annealing of a 5×5 mm^2 SiC sample is shown in Fig. 1, depicting the fast temperature rise and fall rates of the microwave annealing technique.

The surface roughness of the microwave-annealed samples was studied using tapping mode atomic force microscopy (AFM) on 5×5 μm^2 areas. The SiC surface chemistry was studied using sputter profiles of Auger electron spectroscopy (AES) and x-ray photoelectron spectroscopy (XPS). The XPS spectra were acquired using an Mg $K\alpha$ x-ray source and were run at a fixed pass energy. Enough scans were acquired to obtain a reasonable signal-to-noise ratio. Peak fitting was performed using a standard Voigt function. AES experimental details are given elsewhere.[8] Secondary ion mass spectrometry (SIMS) Al depth profiles were performed in a Cameca IMS-4F ion microscope operating with a 5.5 keV net impact energy O_2^+ ion beam and positive secondary ion detection of $^{27}Al^+$ and $^{30}Si^+$. An average relative sensitivity factor (RSF) for Al in SiC was generated from the as-implanted sample based on the stated total dose of 1.35×10^{16} atoms/cm^2, and this RSF was used to determine the Al concentration in all of the annealed samples. The crystallinity and surface stoichiometry of the microwave-annealed samples was evaluated using Rutherford backscattering spectrometry (RBS) coupled with ion-channeling measurements. RBS spectra were acquired at two backscattering angles of 160° and 110°, at a He++ beam energy of 2.275 MeV. For ion-channeling analysis, the beam

TABLE II. rms surface roughness extracted from tapping mode 5×5 μm^2 AFM scans on the Al^+-implanted SiC. The noise level in the measurements is measured to be 0.15 nm.

Anneal schedule (temperature/time)	rms surface roughness (nm)
As implant	0.96
1800 °C/30 s	2.1
1950 °C/30 s	1.7
2050 °C/15 s	2
2050 °C/30 s	1.4

was either aligned with the ⟨0001⟩ axis or otherwise to make a rotating random configuration. Different depth resolutions and backscattering kinematics are afforded by the use of different detection angles. The grazing angle (110°) detector spectra allowed for detailed evaluation of the SiC surface stoichiometry in the microwave-annealed samples. Hall measurements were performed using the van der Pauw technique for electrical characterization of the material after depositing Ni (100 nm) and Ti/Al (20 nm/100 nm) contacts for the P^+- and Al^+-implanted samples, respectively. The contacts were made Ohmic by alloying at 1000 °C for 1 min in 1 atm ultrahigh purity (uhp) argon.

III. RESULTS AND DISCUSSION

A. Atomic force microscopy (AFM) study of the surface morphology

The RMS surface roughness extracted from 5×5 μm^2 tapping mode AFM scans of microwave-annealed Al^+-implanted samples are given in Table II. The rms roughness values for the 1800–2120 °C anneals were in the range of 1.4–2.1 nm. The maximum roughness measured in the microwave annealed samples is 2.1 times the roughness value measured on the as-implanted sample (0.96 nm). The roughness increase in the microwave-annealed samples is much lower than the values observed earlier[12–14] for uncapped conventional furnace anneals (which show an increase in roughness of ~15 times the as-implanted value). The roughness increase after uncapped microwave annealing in this work is comparable to the surface roughness measured earlier after furnace annealing using a graphite[15] or AlN (Ref. 16) cap. These results indicate the attractiveness of a high-temperature short duration annealing.

In this study, no proximity capping was used. Due to this reason, the possibility of redeposition of desorbed Si and C containing species back onto the implanted SiC, resulting in a wavy SiC surface (a mechanism known as step bunching[17–19]), is minimal. A high surface roughness in conventionally annealed SiC is mainly due to the formation of macrosteps caused by the step-bunching effect. Obtaining a low surface roughness for a short duration high-temperature microwave annealing does not mean that there is no sublimation of SiC. As presented later in SIMS results, there is a substantial loss (~100 nm) of implanted SiC with increasing (>2000 °C) annealing temperature.

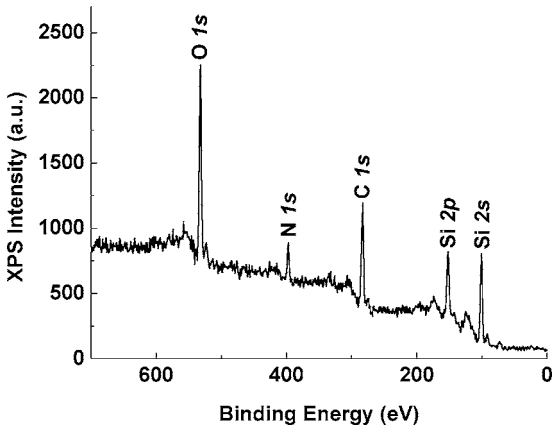

FIG. 2. XPS survey scan for a 1800 °C/15 s microwave-annealed virgin 4*H*-SiC sample.

B. Annealed SiC surface chemical analysis using Auger electron spectroscopy (AES) and x-ray photoelectron spectroscopy (XPS)

Earlier, we have observed that microwave annealing of SiC at temperatures >1800 °C for 15 s in an uncontrolled ambient (air) results in a significant (>100 nm) oxide layer growth.[8] Although the anneals were performed in a controlled (inert) environment in this study, trace amounts of oxygen present in the inert gases may result in the formation of an oxide layer, because the annealing temperatures explored were very high (up to 2100 °C). High-temperature annealing in a N_2 ambient may result in nitridation of the SiC surface. Hence, SiC surface oxidation and nitridation were examined using AES sputter profiling and XPS. All the samples used in this AES and XPS studies were virgin semi-insulating 4*H*-SiC subjected to 15 s microwave annealing at different temperatures.

Figure 2 shows a typical XPS survey scan of a 1800 °C/15 s annealed sample in N_2 ambient. The only elements detected in this survey scan are N, O, C, and Si. Detailed XPS scans indicated that the surface layer is made up of silicon oxide and silicon nitride. The thickness of this surface layer was measured using Auger sputter profiling. It can be seen from Table III that the film thicknesses in the annealed samples ranged from 25–65 Å. As observed in the case of XPS, the AES also indicated the presence of silicon, carbon, nitrogen, and oxygen. Summarizing, the surface film thicknesses measured after microwave annealing in N_2 up to 2100 °C remained <70 Å. This is a marked improvement

TABLE III. Unintentionally formed surface film thickness for 15 s microwave annealing at different temperatures.

Annealing temperature (°C)	Film thickness (Å)
1780	63
1800	33
1900	25
1950	45
2000	25

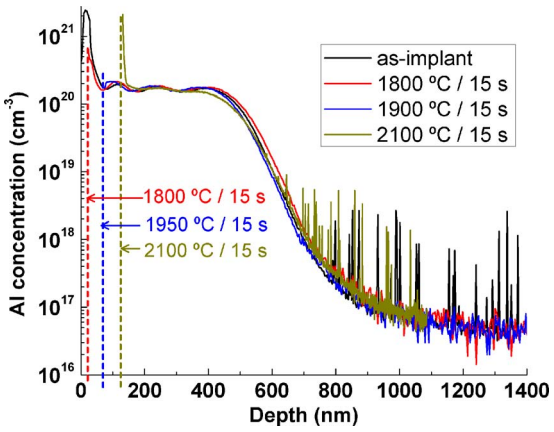

FIG. 3. (Color online) SIMS depth profiles for Al^+-implanted SiC, microwave annealed at 1800, 1950, and 2100 °C for 15 s. After measurements, the profiles were shifted to the right to align the implant tail region with the as-implanted sample. Vertical dotted lines indicate the amount of the implanted region lost during microwave annealing.

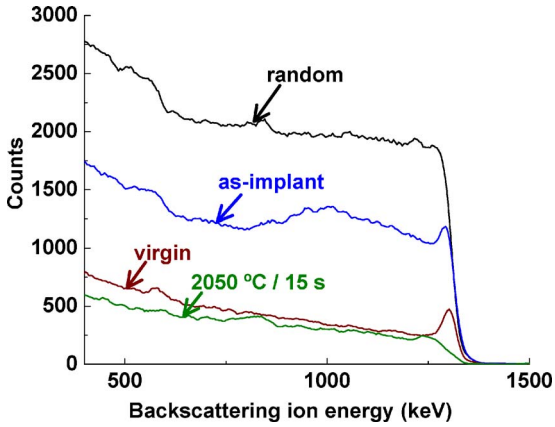

FIG. 4. (Color online) RBS-C aligned spectra for a virgin 4*H*-SiC sample, an Al^+ as-implanted sample, and a 2050 °C/15 s microwave-annealed sample. The RBS-C spectrum for a randomly aligned SiC sample is also shown for reference.

from our earlier study, where the samples annealed in air at temperatures >1850 °C resulted in 1000 Å thick oxide films.[8]

C. Secondary ion mass spectrometry (SIMS) on implanted SiC

It is known that both implanted P and Al are thermally stable in SiC.[20,21] The SIMS measurements in this study were aimed at studying the thickness of the implanted SiC layer lost due to sublimation during microwave annealing. Figure 3 shows an overlay of Al implant depth profiles in as-implanted, 1800 °C/15 s, 1950 °C/15 s, and 2100 °C/15 s annealed samples. In Fig. 3, depth profiles of the annealed samples were shifted to the right to align the implant tail regions of the annealed samples with that of the as-implanted sample. It is very clear that the implant tails have a good match indicating no significant in diffusion of Al. An implant tail matching would not have been possible if Al had in diffused during annealing. From Fig. 3, it is clear that <20 nm of the implanted layer is lost for the 1800 °C/15 s annealed sample, whereas ~120 nm of the implanted layer has sublimed for the 2100 °C/15 s annealed sample.

The sublimation loss of implanted layers during annealing at these high temperatures is expected because no protective cap was used in this study. At present, we are in the process of studying the use of a photoresist-converted graphite cap to minimize the sublimation of the implanted layer during short duration, high-temperature microwave annealing. Preliminary SIMS results on graphite capped samples (not shown) have indicated no surface sublimation of SiC even for a 2100 °C/15 s microwave annealing. However, the application and reliable removal of the graphite cap have to be optimized.[14] Also, the temperature ramping rates of the microwave annealing process may have to be reduced in order to reduce possible thermal stresses at the SiC/graphite cap interface. If the expected loss of the implanted layer is factored in during the design of implanted profiles itself, we may be able to use microwave annealing without any cap. As shown in Table II, the SiC surface sublimation does not result in a dramatic increase in surface roughness.

D. Rutherford backscattering spectrometry channeling (RBS-C) study

The Rutherford backscattering spectrometry channeling (RBS-C) spectra were recorded from the Al^+-implanted SiC samples, before and after microwave annealing. The aligned RBS spectra acquired at a detector angle of 160° were used to study the extent of lattice damage in the samples before and after microwave annealing. Aligned (parallel to the *c* axis) RBS-C spectra of the Al^+-implanted SiC, before and after 2050 °C/15 s microwave annealing, are shown in Fig. 4. For comparison, aligned RBS-C spectra from a virgin SiC sample and a RBS-C spectrum from a randomly aligned SiC sample are also presented in Fig. 4.

In spite of the high implant dose employed, the amorphization of the substrate was avoided due to the elevated implantation temperature (500 °C). The microwave-annealed sample exhibits a scattering yield near the virgin level. This indicates that the high-temperature microwave annealing is very effective in restoring the crystallinity of the implanted SiC.

RBS spectra were also collected (not shown) at a grazing detector angle (110°) to study the impact of the high-temperature microwave annealing on the SiC surface stoichiometry. The analysis of the data collected using both the normal and grazing angle RBS geometries indicated a near perfect (1:1) Si:C ratio from the surface to a depth of ~100 nm in the as-implanted as well as all the microwave-annealed samples. This proves that the short duration, high-temperature microwave annealing preserves the surface stoichiometry of the SiC and prevents the formation of C-rich surface layers.

E. Electrical characteristics of aluminum-implanted 4*H*-SiC

The sheet resistance (R_s) is an important parameter to evaluate the electrical characteristics of an implanted SiC layer because a low R_s can be obtained only if both the sheet

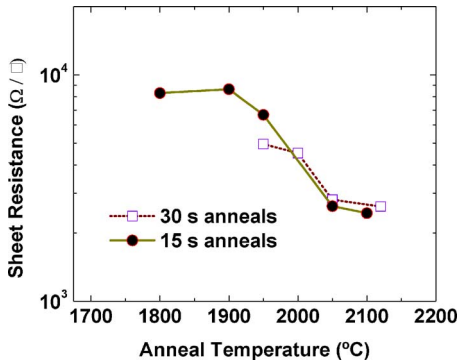

FIG. 5. (Color online) Variation of the sheet resistance with the annealing temperature in Al^+ -implanted 4*H*-SiC, for 15 and 30 s microwave anneals.

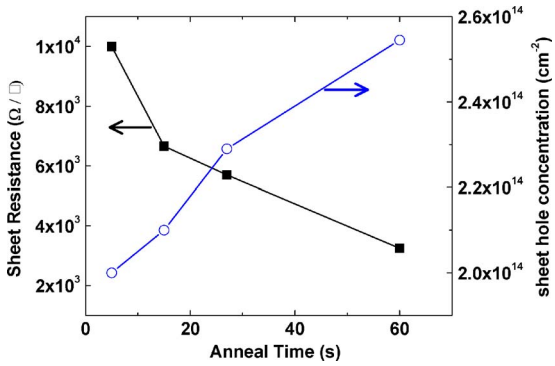

FIG. 7. (Color online) Variation of the sheet resistance and the sheet hole concentration with the annealing time in the Al^+-implanted 4*H*-SiC for 1950 °C annealing.

carrier concentration and carrier mobility are high. Hence, in this work, we present the room temperature (RT) R_s as the prime figure of merit of electrical characteristics of the implanted SiC. Variations of the sheet resistance (R_s) of Al^+-implanted SiC, as a function of the microwave annealing temperature in the range of 1800–2120 °C, for anneal durations of 15 and 30 s, are shown in Fig. 5. Variations of the hole mobility and the sheet hole concentration (p_s) for 15 s anneals, as a function of the annealing temperature, are shown in Fig. 6.

It is clearly seen from Fig. 5 that there is a critical/threshold temperature of 1950 °C above which very low sheet resistances (<5 kΩ/□) are obtained. Microwave annealing at 2100 °C for 15 s yields a sheet resistance of 2.4 kΩ/□. This is among the lowest sheet resistances reported to date for chemically active, acceptor-implanted *p*-type SiC. With increasing annealing temperature, the hole mobility (see Fig. 6) is also found to increase along with a corresponding increase in the sheet hole concentration. The hole mobility attains a maximum value of ~6.8 cm^2/V s for the 2100 °C/15 s annealing. The increase in the hole mobility with the increasing carrier concentration is an indication that the implantation induced defects are annealed out effectively by the high-temperature microwave annealing. This means that the RT hole mobility in the acceptor-implanted material is not primarily limited by ionized impurity scattering (since very few Al atoms are ionized at RT) but rather by

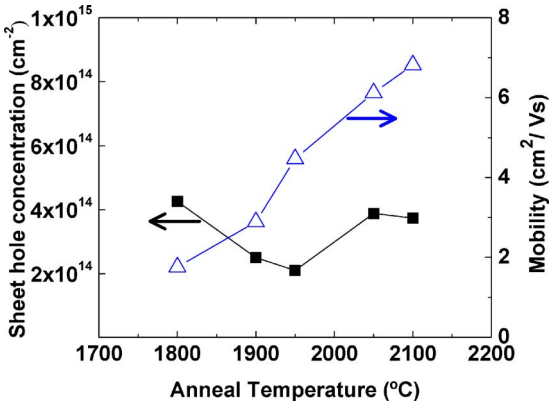

FIG. 6. (Color online) Variation of the sheet hole concentration and hole mobility with the annealing temperature in the Al^+-implanted 4*H*-SiC for 15 s microwave anneals.

defects (residual implantation damage as well as substrate growth related) in the material. The defect concentration in the implanted material continuously decreases with increasing annealing temperature resulting in an increasing hole mobility.

In the past, an extremely high dose (>10^{21} cm^{-3}) Al^+ implantation,[22] with or without flash-lamp annealing,[23] resulted in extremely low resistive layers of SiC. However, the hole mobilties obtained in these layers were extremely low (~0.4 cm^2/V s), implying that either a Mott transition into a metallic phase had occurred or that the low sheet resistivity reported was most likely contributed by the implant-generated high concentration defects, through the so called "hopping conduction" mechanism.[24] In other words, the electrical conduction in these studies was most probably not due to chemically active substitutional dopant activation as observed in the present work.

To elucidate the dependence of electrical characteristics on the anneal time, variations of R_s and p_s as a function of annealing time in the range of 5–60 s are shown in Fig. 7 for an annealing temperature of 1950 °C. There is a drop in the sheet resistance and a corresponding increase in sheet carrier concentration, with an increasing annealing time. The hole mobilities were again in the range of 3–7 cm^2/V s, which is an indicator of chemically activated electrical conduction.

Microwave annealing resulted in an increasing sheet carrier concentration with increasing annealing temperature (upto 2050 °C) and increasing anneal duration in spite of losing a portion of the implanted layer due to sublimation. If this sublimation rate is factored into the results, the increasing sheet carrier concentration with increasing annealing temperature is much more impressive than indicated by Figs. 6 and 7.

F. Electrical characteristics of phosphorus-implanted 4*H*-SiC

Variations of the sheet resistance (R_s) and the sheet electron concentration (n_s) of the phosphorus-implanted material with the microwave annealing temperature, in the range of 1700–1950 °C, for an anneal duration of 30 s, are shown in Fig. 8. A corresponding plot of the electron mobility is shown in Fig. 9.

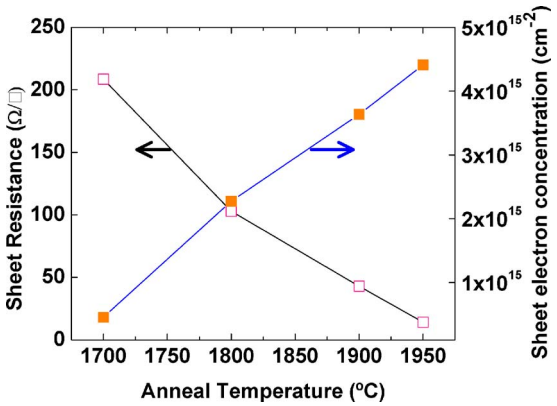

FIG. 8. (Color online) Variation of the sheet resistance and the implant sheet carrier concentration with the annealing temperature in the P^+-implanted 4*H*-SiC, for 30 s anneals.

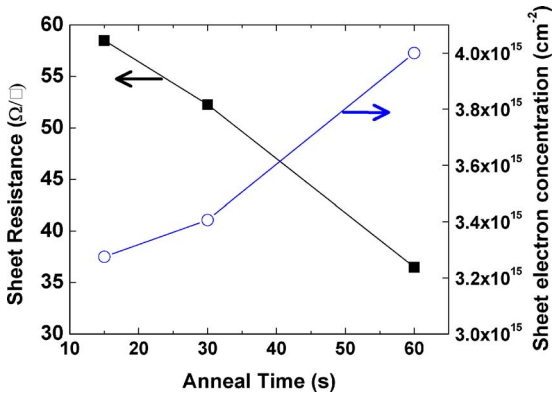

FIG. 10. (Color online) Variation of the sheet resistance and the sheet electron concentration with the annealing time at 1925 °C for the P^+-implanted 4*H*-SiC.

It can be observed from Fig. 8 that microwave annealing at temperatures $\geqslant$1900 °C for 30 s yields ultralow sheet resistances ($<$50 Ω/□) combined with high sheet electron concentrations. Microwave annealing at 1950 °C for 30 s resulted in an unprecedented sheet resistance of 14 Ω/□ accompanied by a sheet electron concentration of 4.4×10^{15} cm^{-2} and an electron mobility of 100 cm^2/V s. High sheet electron concentrations measured in this study are possibly due to the high phosphorus doping concentration (2×10^{20} cm^{-3}), which exceeds the N_c (conduction band density of states) value for 4*H*-SiC (1.35×10^{19} cm^{-3}), resulting in an impurity band formation under the conduction band and a subsequent reduction in the carrier ionization energy. The combination of high carrier mobility and high sheet electron concentration is a clear indication of the alleviation of the implant-generated defects.

To elucidate the dependence of electrical characteristics on the anneal time, the variation of R_s and n_s with annealing time in the range of 15–60 s, at a temperature of 1925 °C is shown in Fig. 10. There is a drop in the sheet resistance and a corresponding increase in the sheet carrier concentration, with an increasing annealing time. For a similar phosphorus doping concentration, Senzaki *et al.*[25] observed a decrease in n_s with increasing annealing time for 1700 °C annealing. They attributed this behavior to the precipitation of P donors, which leads to effective carrier density lowering. Upon comparing Figs. 8 and 10, it can be concluded that for P^+ implantation the electrical characteristics show a much weaker dependence on the anneal time compared to the annealing temperature.

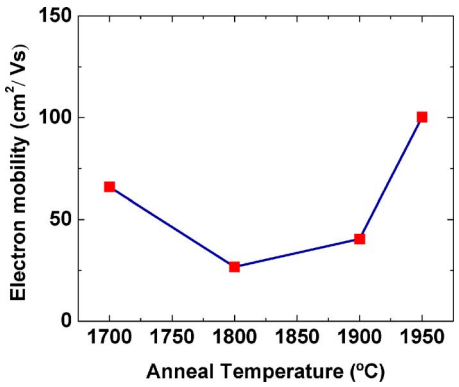

FIG. 9. (Color online) Variation of the electron mobility with the microwave annealing temperature for the P^+-implanted 4*H*-SiC.

IV. CONCLUSIONS

Solid-state microwave annealing is an attractive method for rapid thermal annealing of implanted SiC. Using this technique, annealing temperatures as high as 2100 °C can be reached with a ramp-up rate of $>$600 °C/s and a fall rate of 400 °C/s. The rms surface roughness after uncapped microwave annealing at 2050 °C for 30 s in N_2 ambient is comparable to the surface roughness of the capped samples subjected to the conventional annealing at 1700 °C. SIMS depth profiles show negligible Al in diffusion even at annealing temperatures as high as 2100 °C. However, a sublimation of 120 nm of the SiC surface layer is noticed upon annealing at 2100 °C for 15 s. We are in the process of performing anneals on graphite capped SiC samples, in order to minimize surface sublimation. The initial results are promising for graphite-capped anneals at 2100 °C for 15 s. The lattice quality of the microwave-annealed material is near the virgin SiC, indicating the complete removal of implantation-induced damage. Electrical characterization of both Al^+-and P^+-implanted materials subjected to microwave annealing yielded very low sheet resistance and high carrier mobility values. This is again an indication that the microwave annealing is effective in both activating the implanted dopants and reducing the implantation generated defects in the SiC material.

ACKNOWLEDGMENTS

We are grateful to Dr. A.V. Davydov of NIST for letting us use NIST facilities and Dr. E. Gomar-Nadal of the University of Maryland for her help with some AFM measurements. The GMU work is supported by Army Research Office (Dr. Prater) under Grant No. W911NF-04-1-0428 and a subcontract from LT Technologies under NSF SBIR Grant No. 0539321.

[1]T. P. Chow and M. Ghezzo, Mater. Res. Soc. Symp. Proc. **423**, 9 (1996).
[2]H. Matsunami, Jpn. J. Appl. Phys., Part 1 **43**, 6835 (2004).

[3]G. L. Harris, H. S. Henry, A. Jackson, and S. Yoshida, in *Properties of Silicon Carbide*, edited by G. L. Harris (INSPEC, IEEE, London, UK, 1996), Chap. 3, pp. 63–81.
[4]O. Kordina and S. E. Saddow, in *Advances in Silicon Carbide Processing and Applications*, edited by S. E. Saddow and A. Agarwal (Artech House, Norwood, MA, 2004), Chap. 1, pp. 1–4.
[5]M. V. Rao, Solid-State Electron. **47**, 213 (2003).
[6]A. Hallen, R. Nipoti, S. E. Saddow, S. Rao, and B. G. Svensson, in *Advances in Silicon Carbide Processing and Applications*, edited by S. E. Saddow and A. Agarwal (Artech House, Norwood, MA, 2004), Chap. 4, pp. 109–148.
[7]M. V. Rao, J. B. Tucker, M. C. Ridgway, O. W. Holland, N. Papanicolaou, and J. Mittereder, J. Appl. Phys. **86**, 752 (1999).
[8]S. G. Sundaresan, Y.-L. Tian, J. A. Schreifels, M. C. Wood, K. A. Jones, A. V. Davydov, and M. V. Rao, J. Electron. Mater. (to appear).
[9]T. Troffer, C. Peppermuller, G. Pensl, and A. Schoner, J. Appl. Phys. **80**, 3739 (1996).
[10]J. A. Gardner *et al.*, J. Appl. Phys. **83**, 5118 (1998).
[11]E. M. Handy, M. V. Rao, O. W. Holland, P. H. Chi, K. A. Jones, M. A. Derenge, R. D. Vispute, and T. Venkatesan, J. Electron. Mater. **29**, 1340 (2000).
[12]M. A. Capano, S. Ryu, M. R. Melloch, J. A. Cooper, Jr., and M. R. Buss, J. Electron. Mater. **27**, 370 (1998).
[13]M. Rambach *et al.*, Nucl. Instrum. Methods Phys. Res. B **237**, 68 (2005).
[14]M. A. Capano *et al.*, J. Electron. Mater. **28**, 214 (1999).
[15]K. V. Vassilevski *et al.*, Semicond. Sci. Technol. **20**, 271 (2005).
[16]K. A. Jones *et al.*, Mater. Sci. Eng., B **61–62**, 281 (2000).
[17]M. A. Capano, S. Ryu, M. R. Melloch, J. A. Cooper, Jr., and M. R. Buss, J. Electron. Mater. **27**, 370 (1998).
[18]K. Hata, A. Kawazu, T. Okano, T. Ueda, and M. Akiyama, Appl. Phys. Lett. **63**, 1625 (1993).
[19]V. R. Vathulya and M. H. White, Solid-State Electron. **44**, 309 (2000).
[20]T. Troffer, M. Schadt, T. Frank, H. Itoh, G. Pensl, J. Heindl, H. P. Strunk, and M. Maier, Phys. Status Solidi A **162**, 277 (1997).
[21]G. Pensl *et al.*, Inst. Phys. Conf. Ser. **142**, 275 (1996).
[22]Y. Negoro, T. Kimoto, H. Matsunami, F. Schmid, and G. Pensl, J. Appl. Phys. **96**, 4916 (2004).
[23]H. Wirth, D. Panknin, W. Skorupa, and E. Niemann, Appl. Phys. Lett. **74**, 979 (1999).
[24]W. C. Mitchel, A. O. Evwaraye, S. R. Smith, and M. D. Roth, J. Electron. Mater. **26**, 113 (1997).
[25]J. Senzaki, K. Fukuda, and K. Arai, J. Appl. Phys. **94**, 2942 (2003).